The final publication is available at

https://doi.org/10.1016/j.triboint.2019.105985

Additional Information

On the Use of the Theory of Critical Distances with Mesh Control for Fretting Fatigue Lifetime Assessment

A. Zabala[1,*], D. Infante-García[2], E. Giner[3], S. Goel[4], J. L. Endrino[5,6], I. Llavori[1]

[1]*Surface Technologies, Mondragon University, Loramendi 4, 20500 Arrasate-Mondragon, Spain*

[2]*Dept. of Mechanical Engineering, University Carlos III of Madrid, Avda. de la Universidad 30, 28911 Leganes, Madrid, Spain.*

[3]*Centre of Research in Mechanical Engineering - CIIM, Dept. of Mechanical Engineering and Materials, Universitat Politècnica de València, Camino de Vera, 46022 Valencia, Spain.*

[4]*School of Aerospace, Transport and Manufacturing, Cranfield University, Bedfordshire, MK430AL, UK*

[5]*Basque Center for Materials, Applications & Nanostructures, UPV/EHU Science Park, Barrio Sarriena s/n, 48940 Leioa, Spain*
[6]*IKERBASQUE, Basque Foundation for Science, Maria Diaz de Haro 3, 48013 Bilbao, Spain*

*Corresponding author: azabalae@mondragon.edu (Alaitz Zabala)

ABSTRACT

This work analyses the viability of the theory of critical distances (TCD) using mesh control for fretting fatigue lifetime assessment. More than seven hundred sets of simulations were performed by taking seventy different experimental tests reported previously in the literature. The outcome of the present study suggests that the TCD mesh control method can be extended to fretting fatigue problems by the reasonable assumption of setting the right element size proportional to critical distance. In this study, a significant computational time reduction of up to 97% was obtained. Thus, this study provides a simple method to design complex 3D industrial components subjected to fretting fatigue phenomena using finite element analysis efficiently without requiring complex remeshing techniques.

KEYWORDS. Fretting fatigue, Theory of Critical Distances (TCD), finite element analysis.

Nomenclature

Abbreviations

DoE	= Design of experiment
FEA	= Finite Element Analysis
FEM	= Finite Element Method
FFM	= Finite fracture mechanics
FIP	= Fatigue Indicator Parameter
FS	= Fatemi-Socie
ICM	= Imaginary crack method
LM	= Line Method
MC	= Mesh Control
MPC	= Multi-point constraint
PM	= Point Method
PS	= Point Stress
SWT	= Smith-Watson-Topper
TCD	= Theory of Critical Distances

Symbols

|	
A	= Cross section area
d	= Element size
N_A	= Reference number of cycles to failure
L	= Critical Distance
P	= Normal force
Q	= Tangential Force
r_{pad}	= Pad radius
R_σ	= Fully reversed bulk stress
R_Q	= Fully reversed tangential force
σ_B	= Bulk stress
σ_R	= Bulk stress reaction
σ_0	= Fatigue limit
$\Delta\sigma_0$	= Fatigue limit range
ΔK_{th}	= Fatigue crack propagation threshold

1. Introduction

Fretting phenomena arise when two bodies that are in contact are subjected to relative movement of small amplitude (0–300 μm), producing damage on the contact surface [1] that can lead to catastrophic failure. When the presence of fretting is in conjoint action with cyclic remote loading, this reduces the fatigue performance and the effect is known as fretting fatigue [2].

Since virtually all machines vibrate, many engineering assemblies (even ones that are not intended to move) are prone to fretting fatigue problems, including aircraft engine blade housings [3], ropes [4], flexible couplings [5], self-piercing rivets [6] and even orthopaedic devices [7]. Consequently, fretting fatigue presents major safety and economic concerns. Predicting this phenomenon is of major importance in determining, for instance, the lifetime of safe use of critical components. However, despite numerous advances made in this area, there is no general model that can predict fretting fatigue.

The use of the finite element method (FEM) to analyse fretting fatigue phenomena has attracted interest, since it provides valuable failure data that is very difficult to capture via direct experiments and/or analytical solutions [8]. The major difficulties in dealing with fretting fatigue simulation arises from (i) the intense stress gradient below the contact surface in the vicinity of the contact edge [9], and (ii) the multiaxial and non-proportional nature of the loading conditions [10].

Due to the localized stress at the surface, local approaches based on estimating the stresses at the hot spots (see **Fig. 1**) are not appropriate for predicting fretting fatigue lives, since they provide over-conservative results [11]. Thus, non-local methods are more appropriate for life prediction in the presence of high stress gradients, such as the ones existing in fretting fatigue contacts [12–15].
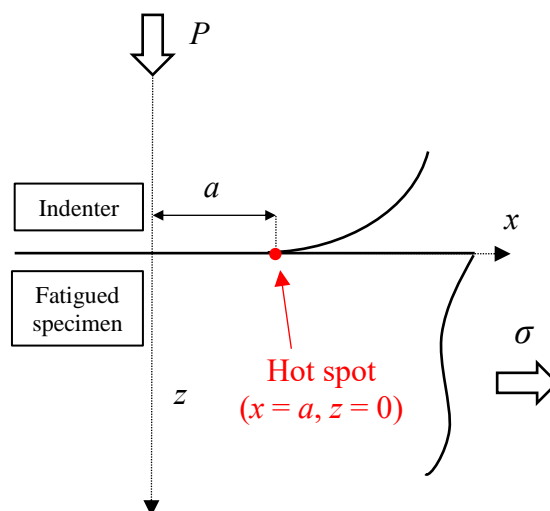
Fig. 1. Schematic description of the hot spot (i.e., the edge of the contacting surfaces in fretting fatigue).

The theory of critical distances (TCD) [16] is the name given to a group of methods and has been one of the most widely used non-local approaches over the last decade, and was introduced in the fretting literature [17,18] to predict notch fatigue effects or those caused by stress concentrators.

The TCD has been applied to predict notch-based fracture and fatigue in a wide range of materials and components [19]. Taylor considers four methods, the point method (PM), line method (LM), imaginary crack method (ICM), and finite fracture mechanics (FFM), to be different manifestations of the same TCD method, as all these methods reveal a very similar result. All the methods have certain features in common: (i) the use of a characteristic material length parameter, the so-called critical distance L, and (ii) the fact that all are based on linear elastic analysis. The point method (PM) is the simplest form of the TCD and, therefore, the most convenient for industrial components. The criterion is stated as follows: 'Failure will occur when the stress at a distance $L/2$ from the notch root is equal to σ_0' [16], and can be written as:

$$\sigma(L/2) = \sigma_0,\tag{1}$$

where L is the so-called critical distance, the stress at a distance $L/2$ is the point stress (PS) and σ_0 is the fatigue limit. The value of L is a material constant which can be found either by conducting tests on notched specimens or by using the following relationship: :

$$L = \frac{1}{\pi}\left(\frac{\Delta K_{th}}{\Delta \sigma_0}\right)^2,\tag{2}$$

where $\Delta \sigma_0$ is the fatigue limit range and ΔK_{th} is the fatigue crack propagation threshold. Usually, a fully reversed loading ratio is used for $\Delta \sigma_0$ in fretting, as the fretted contact introduces compressive stresses. On the other hand, a zero loading ratio ($R=0$) is used for ΔK_{th}, since it is assumed that compressive stresses do not contribute to crack propagation [10].

In the early 1950s, when the TCD method was developed for the prediction of metal fatigue, it was daunting to obtain accurate stress-field data for components, so their industrial use required over-simplified empirical equations. However, the use of these equations and their subsequent refinements is now inappropriate, particularly when finite element analysis (FEA) can reveal much more clarity about the stress field near sharp features. However, a FEA of this sort of problem currently relies on a cumbersome trial and error way of asserting an appropriate meshing strategy.

For example, the first problem concerns the required mesh refinement. Mesh must be fine enough to provide an accurate picture of the stress field in the region of interest at a distance $L/2$ from the feature. Due to the extremely localized stress gradients present during fretting fatigue phenomena, the contact interface requires an extra fine mesh [20,21]. On the other hand, the method requires obtaining stress values inside the body, which is a time-consuming activity, and one that is difficult to automate.

More recently, Vargiu et al. [22] proposed an alternative approach, TCD with mesh control, which was applied to notched specimens to overcome the limitations seen with TCD methods. The rationale behind the proposed method relies on the hypothesis that it is possible to pre-set the element size to be the multiple of L critical distance such that the hot-spot stress obtained from the simulation can be used in place of the PS in the normal TCD point method (see **Fig. 2**).
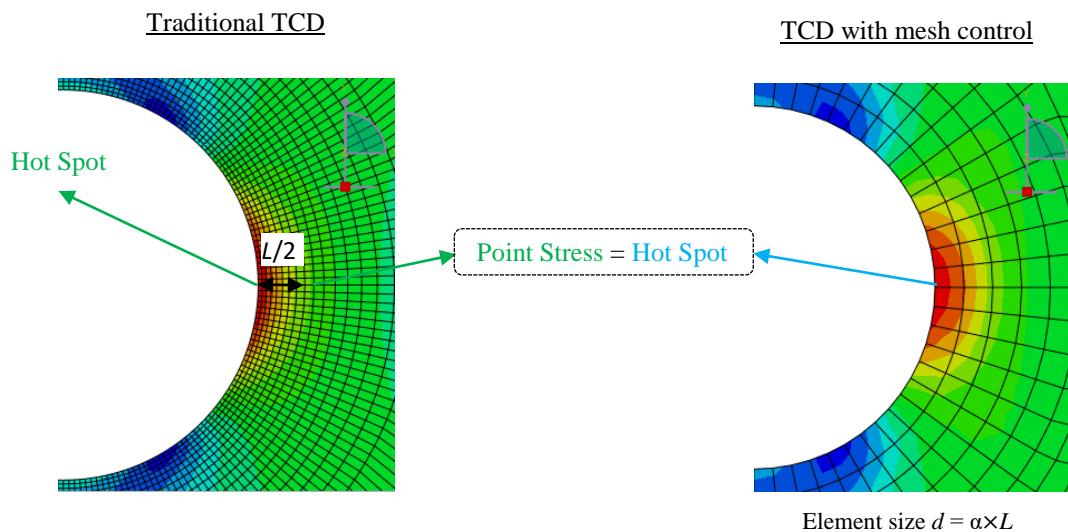
Fig. 2. Schematic illustration of the TCD with mesh control concept

This approach potentially avoids two problems: (i) a relatively coarser mesh can be used and (ii) there is no need to obtain path information to find the PS. This approach was tested using seven different notch types, and an acceptable accuracy with errors less than 20% when comparing to the original TCD Point Method approach was obtained [22].

Previous works have analysed different methods to deal with the presence of high stress gradients in fretting fatigue by using a characteristic length to average the stresses under the contact along a line or over a volume. For instance, Fouvry et al. [23] used an average of Dang Van's fatigue criterion [24] over a critical volume to predict the experimental fretting fatigue performance of Ti-6Al-4V. The optimal critical volume was found to be 5 μm^3. Araújo and Nowell [25,26] analysed the behaviour of the same alloy applying the Smith-Watson-Topper [27] (SWT) and Fatemi-Socie [28]

(FS) criteria. They found that the average volume required to fit the experimental observation was on the order of 5 to 20 µm^3. Regarding the Al/4%Cu alloy, a cubic of about 50 µm provided the best fit to the results.

Earlier, Bernardo et al. [17] proposed the use of the finite element itself as the process volume. By modifying the element size on the x and y axes, they found that the choice of an appropriate mesh refinement level and element size is able to successfully predict the experimental data. Those studies suggest that volumetric averaging methods could be a suitable strategy to deal with stress gradients present in fretting fatigue; however, these methods need experimental validation.

The aforementioned approach of TCD with mesh control, while similar in concept, would present an advance in the fretting field due to the simplicity of its implementation. This procedure has so far been tested for notched specimens under proportional stress loading cases, but has not been tested for its application to fretting fatigue analysis. The fact that high-strength materials subjected to fretting fatigue phenomena tend to have small critical distance values increases the benefits of applying this methodology to fretting fatigue phenomena.

Therefore, the present study aims to analyse the viability of using the TCD mesh control approach for fretting fatigue life prediction. With this objective, the optimum mesh size for fretting fatigue analysis was evaluated by first conducting a theoretical study using synthetic critical lengths, and later verified by analysing seventy varying experimental test conditions. The suitability of the selected optimum mesh size for fretting fatigue lifetime assessment was then evaluated comparing the obtained results with reported experimental data.

2. Methodology

2.1 Analysis scheme

The traditional way of implementing the TCD by using the PM is to analyse the stresses and strains at a distance of $L/2$ from the surface. To accurately define the stress field at the PS, a very fine mesh size is needed. In this study, the element size was set to be at least four times less than the value of L in order to obtain robust stress values [29]. On the other hand, the mesh control approach chooses an element size d relative to L so that the FEA hot spot result is equal to the PS value of the traditional TCD method. As mentioned in the introduction, this approach overcomes the computational time problem due to the small element size needed in fretting fatigue cases, and it also eliminates the need

to obtain path information to find the PS, which is otherwise challenging because of the need to simulate complex geometry parts.
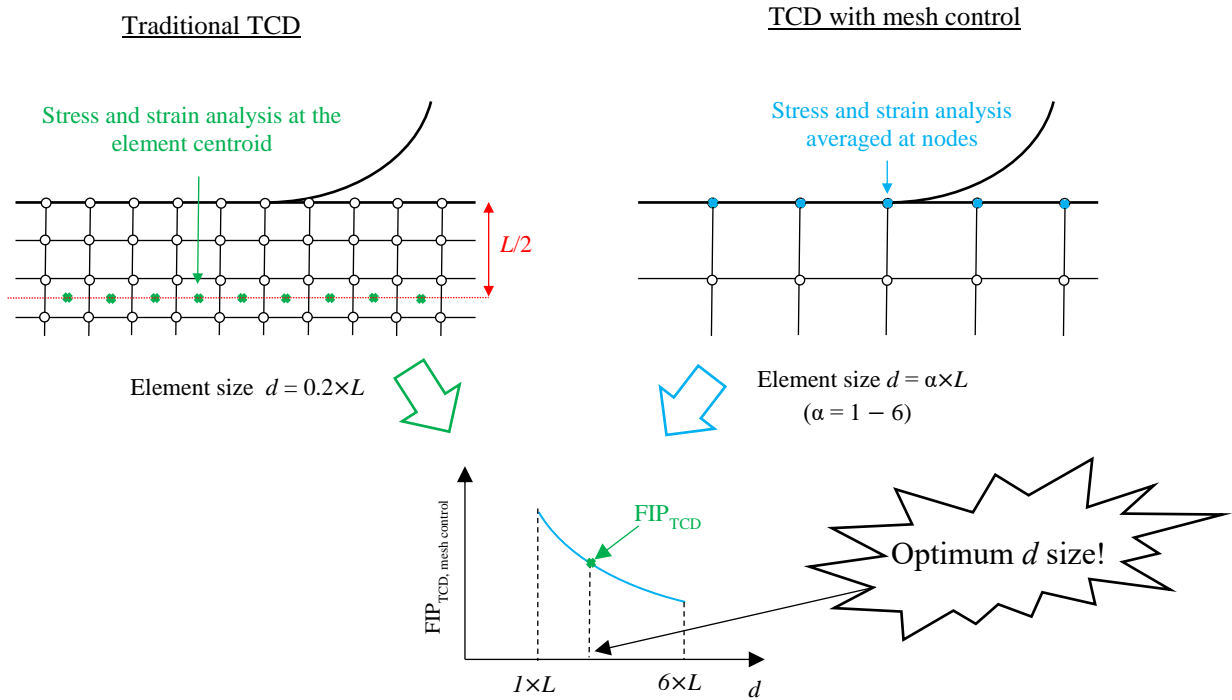
Fig. 3. Adopted analysis scheme to define the optimum element size d via the TCD with the mesh control method. FIP$_{TCD}$= fatigue indicator parameter, calculated using the TCD with the mesh control method.

In this study, the element size d was set to $L/5$ for the traditional TCD, and in each case the stresses were recorded at the centroids of the third element layer, which are between the third and fourth nodes from the surface at a distance of $L/2$ (see **Fig. 3**). In the case of the mesh control approach, the element size was modified between $1 \times L$ and $6 \times L$, and each fatigue indicator parameter (FIP, further described in Section 2.4) result was compared to the target value (which corresponds to the original TCD method result). This way, the optimum d size (corresponding to a minimum error) was defined for each case. One important point to be considered in this procedure is related to the scheme used to translate the stresses from the integration point to the nodes. Each FEA commercial software package has its own technique and the results may vary from software to software. In this study, the *averaged at nodes* technique available in Abaqus FEA was used.

### 2.2. Summary of experimental data taken from the literature

Experimental data regarding fretting fatigue under cylindrical contacts was taken from the literature that represents a broad range of test conditions of high strength aluminium and titanium alloys commonly used in the aerospace industry. In all cases, the cylindrical pads were pushed against a rectangular dog-bone specimen and a constant amplitude bulk stress was applied to the specimen, as shown in **Fig. 4**. A tangential force Q was therefore generated between the cylindrical pad and the dog-bone specimen.

The first set of experimental data considered in the present study was performed by Szolwinski and Farris [30] on a single hydraulic actuator machine using Al2024-T351 alloy. Those experiments were carried out in a partial slip regime with the bulk stress and tangential force being fully reversed ($R_\sigma =$ -1 and $R_Q =$ -1). In order to study the interaction effects between the variables, they performed several experiments following the design of experiments (DoE) method. A total of four independent variables were considered for DoE, namely (i) the normal force P, (ii) the bulk stress σ_B, (iii) the ratio between the maximum tangential force Q_{max} and normal force P, and (iv) the pad radius r_{pad}.

The second experimental data set was generated by Talemi et al. [31] on a 100 kN EHS servo hydraulic machine. Talemi et al. [31] employed an aluminium 2024-T3 alloy and the only variable considered by them was the bulk stress with a positive ratio ($R_\sigma = 0.1$). In each test, the tangential force Q was seen to be proportional to the cyclic remote stress and fully reversed ($R_Q =$ -1).

The third experimental data set was from the work of Nowell [32] on Al/4%Cu who performed four different series of experiments to analyse the influence of the contact half width a, the maximum normal pressure p_0, the fully reversed tangential force, and the fully reversed bulk stress on fatigue life.

The last experimental data set was produced by Araujo and Nowell [25] on Ti-6Al-4V. In this case, the only variable considered was the contact width with five different pad radii. The fatigue specimen was cycled between 0.9 MPa and 280 MPa. **Table 1** and **Table 2** summarise the test conditions and the material properties of the reported data.
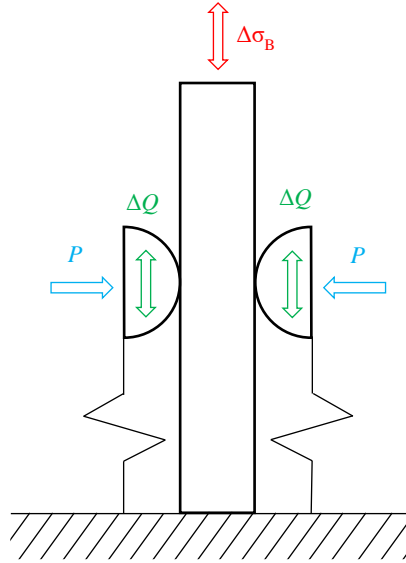
Fig. 4. Typical fretting fatigue test rig sketch.

Table 1. Summary of the experimental data *[25,30–32]*.

Material	σ_{bulk} [MPa]	Q_{max}/P [-]	P [N]	p_0 [MPa]	r_{pad} [mm]	a [mm]
Al2024-T351	81-115.8	0.21-0.52	5201-7226	154-240	127-229	1.21-2.01
Al2024-T3	100-220	0.29-0.59	543	135.75	50	0.92
Al/4%Cu	77.2, 92.7	0.45	291-3497	120-157	12.5-150	0.1-1.14
Ti-6Al-4V	280	0.16	3237-18130	650	12.5-70	0.25-1.42

Table 2. Material properties *[25,30–32]*.

Material	Elastic modulus E [GPa]	Poisson's ratio v [-]	Coefficient of friction μ [-]
Al2024-T351	74.1	0.33	0.65
Al 2024-T3	72.1	0.33	0.65
Al/4%Cu	74	0.33	0.75
Ti-6Al-4V	115	0.32	0.55

2.3. Fatigue and critical distances input data

Table 3 presents the material fatigue constants of the materials obtained from the published literature. The corresponding critical distance values *L* were computed using the previously shown Eq. 2.

Table 3. Adopted plain fatigue and fracture data. <mark>Note: N_A is the reference number of cycles to failure.</mark>

| Material	Ref.	σ_f' [MPa]	b [-]	ΔK_{th} ($R=0$) [MPa·m$^{1/2}$]	$\Delta\sigma_0$ ($R=-1$) [MPa]	N_A [Cycles]	L [µm]
Al 2024-T351	[10,33]	714	-0.078	2.1	235	$5\cdot10^8$	25.42
Al 2024-T3	[31,34,35]	1194	-0.133	3.2	276	$5\cdot10^8$	42.79
Al/4%Cu	[25,35]	1015	-0.11	2.1	248	$5\cdot10^8$	22.82
Ti-6Al-4V	[10,36,37]	2030	-0.104	4.2	569	ND	17.34

2.4. Fatigue indicator parameter

In fretting fatigue under incomplete contact, shear stress and normal pressure tend to zero at the crack initiation zone (trailing edge of the contact). Accordingly, a mode I-based fatigue indicator parameter was selected for the study. The SWT [27] multiaxial fatigue criterion within the critical-plane approach was chosen to estimate the location and number of cycles to failure,

$$SWT = \sigma_{n,max}\varepsilon_{n,a} = \frac{\sigma_f'^2}{E}\left(2N_f\right)^{2b},$$ (3)

where $\sigma_{n,max}$ is the maximum normal stress within a fretting cycle, $\varepsilon_{n,a}$ is the normal strain amplitude (both with respect to the critical plane), N_f is the number of cycles to failure, σ_f' is the fatigue strength coefficient, and b is the fatigue strength exponent. <mark>The plastic part of the equation was not considered based on the fact that the experimental tests were performed under elastic assumption, and its contribution was considered negligible.</mark>

2.5. FE modelling

The finite element model was developed in Abaqus FEA as a 2D plane strain model similar to [31], using quadrilateral elements (CPE4). **Fig. 5** illustrates a conceptual sketch of the FE model, with an example of (a) boundary condition (b) and load sequence, which were tailored for each particular case used in this study.

$$(a) \qquad\qquad\qquad\qquad (b)$$
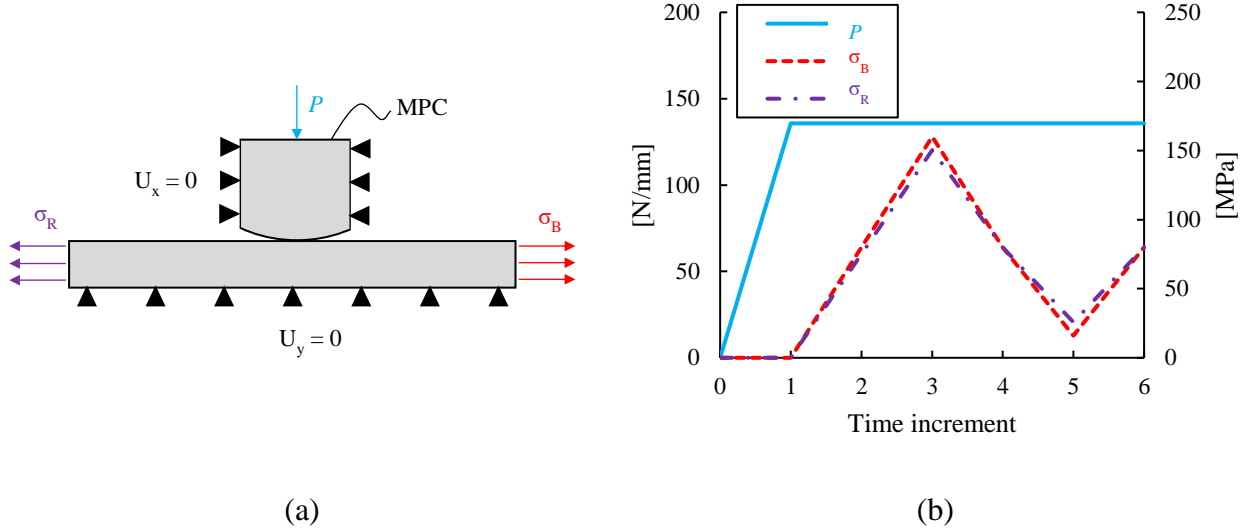
Fig. 5. Sketch of FE model: (a) boundary conditions; (b) loading sequence for test FF5 of Talemi et al. [31]
Note: MPC refers to multi-point constraints.

It should be highlighted here that the bulk stress reaction σ_R for each time increment was calculated using the following equation:

$$\sigma_{R,i} = \sigma_{B,i} - Q_i/(A/2), \tag{4}$$

where A is the cross-section area of the fatigue specimen and the subscript i denotes the time increment.

3. Results and discussion

3.1 Synthetic L data analysis

The value of the critical distance (L) has a strong influence on the lifetime predictions due to the severe stress gradients found under fretting fatigue conditions. In addition, L may influence the optimum mesh size when the TCD is applied in combination with the mesh control (MC) method, as is proposed in this study. Thus, a parametric study with different synthetic critical distance values has been performed to assess the influence of L on the optimum mesh size when applying TCD with MC. The study has been performed on the FF5 loading condition of the results reported by Hojjati-Talemi et al. [31]. As mentioned earlier, **Table 1** and **Table 2** summarize the loading details and material properties, respectively

The critical distance values tested in this study (10, 30, 50, 70 and 100 microns) cover a wide range of L values found in high-strength materials typically employed under fretting fatigue conditions.

First, the target value was set for each L value following the traditional TCD methodology. To that end, the SWT parameter was calculated at $L/2$ from the hot spot using a mesh size of $0.2 \times L$. Next, the SWT parameter was directly calculated at the hot spot using 10 different meshes with an element size d equal to $\alpha \times L$ for each L value, being α in a range from 1 to 6, as proposed in the TCD with MC methodology [22]. Finally, the optimum mesh size value is found for each synthetic L value. **Fig. 6** shows the relative mean error in SWT obtained with MC with respect to the traditional TCD for L values of 10, 30, 50 and 70 (bars represent the maximum and minimum relative error).
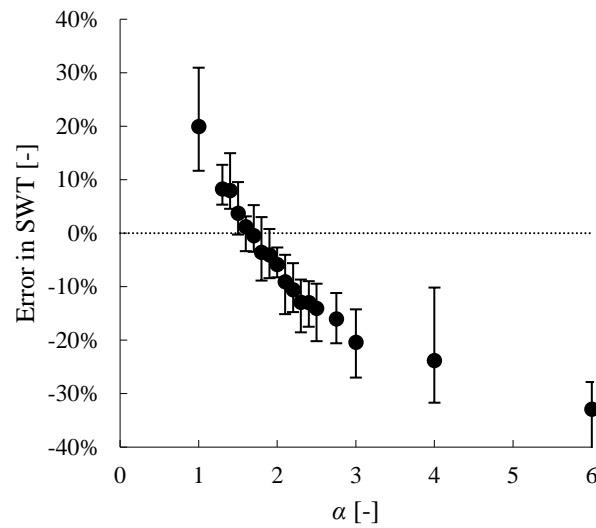
Fig. 6. Summary of the mean predicted relative errors obtained with the TCD method with mesh control with respect to the traditional TCD method for different element sizes and for all the synthetic studied L values (10, 30, 50 and 70 µm). Note: Errors are expressed as mean values and bars representing the minimum and maximum values in order to illustrate the entire range of the error that could occur for each element length considering all cases.

As can be seen in **Fig. 6**, a smaller SWT value was obtained while using a coarse mesh, due to the larger averaging effect of the stress gradient. Conversely, erratic behaviour was observed for the simulations while using a very large critical distance of $L = 100$ µm (see **Fig. 7** (a)).
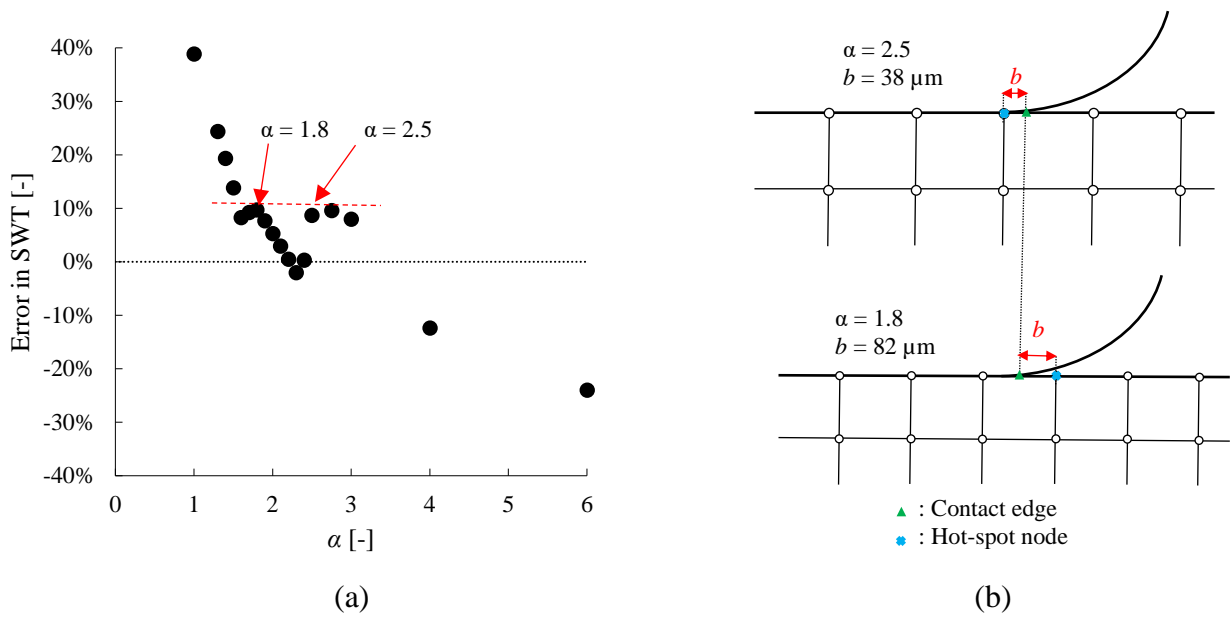
Fig. 7. Erratic behaviour observed for simulations using large critical distance of L = 100 µm. (a): Relative errors of the TCD with mesh control with respect to the traditional method for different element sizes (case of synthetic L = 100 µm). Nodes with different element size show the same relative error in SWT. (b): Schematic description of the two cases pointed out in the graph where b is the distance from the contact edge to the hot spot node.

The main reason for this erratic behaviour is that the relative position of the hot spot node with respect to the contact edge begins to dominate over the mesh size when using large L values. **Fig. 7** (b) shows an example of two cases presenting different element sizes and providing the same SWT values. As can be observed, even if the bigger element size would be expected to provide a smaller SWT value (due to the greater averaging), it reports the same value since the hot spot node is closer to the contact edge. Therefore, the case of L equal to 100 microns was excluded from the present study, and the following corresponds only to the results shown in **Fig. 6**.

The mean optimum mesh size found was $1.6 \times L$, giving a mean relative error of 2.9% and a maximum relative error of 3.4% when compared to the traditional TCD method. It should be noted that the optimum mesh size for each L size ranged from $1.5 \times L$ to $1.9 \times L$, bringing the relative error lower to 1% in all cases. Thus, the predictions can be further improved if the optimum mesh size is evaluated for each L size individually.

Due to the fact that the aim of the study was to analyse the viability of the proposed method that can be applied in an industrial framework, the use of a mean optimum mesh size for all cases was preferred, since a maximum relative error of 4% seems to be acceptable. Accordingly, a mesh size of $1.6 \times L$ was selected to test the comparison with experimental data.

3.2 Reported experimental L data analysis

In order to test the robustness of the method, the same procedure described in section 3.1 was carried out with the reported experimental tests described in section 2.2. In total, seven hundred simulations were carried out, corresponding to seventy experimental tests analysed with ten different mesh sizes each.

In **Fig. 8**, a summary of the relative mean error in SWT obtained with the MC method is depicted for different mesh sizes. Trends similar to those observed in section 3.1 were obtained, revealing the minimum error using an element size $d = 1.6 \times L$. In all cases, the mean error was below 5%, and the maximum error was below 12%. It is noteworthy that the time reduction when using the MC as compared the traditional method was up to 97% for the optimum element size of $1.6 \times L$, which is a considerable decrease in computational requirements.

(a)   (b)
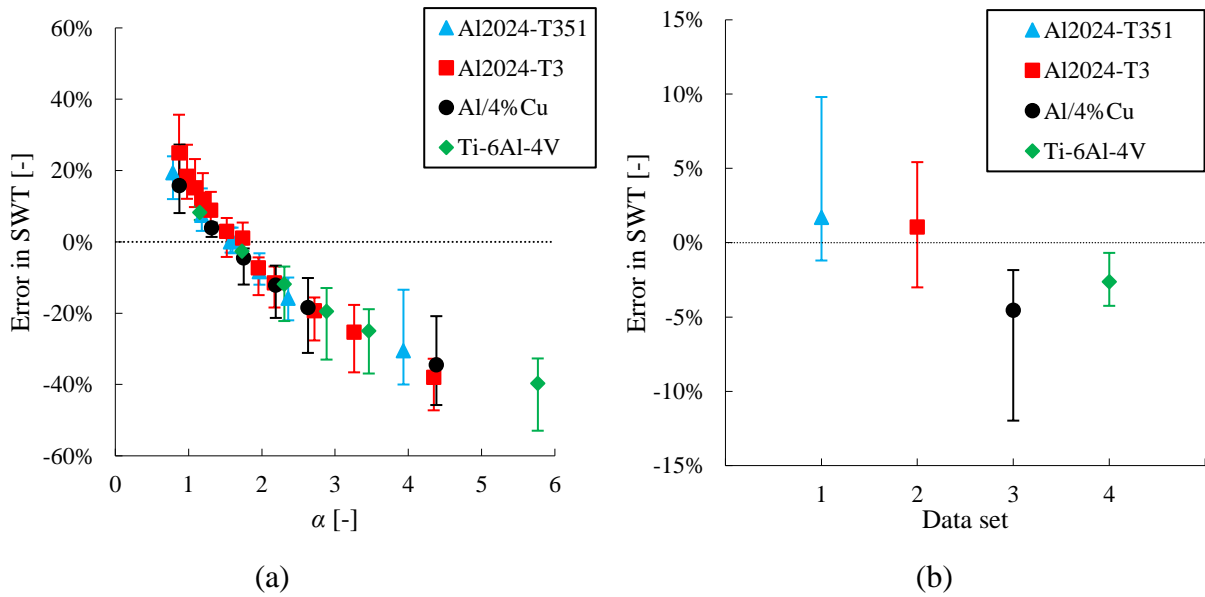
Fig. 8. (a) Summary of the predicted errors obtained with the TCD with mesh control method for all cases under study at different element sizes calculated as a percentage change with respect to the traditional TCD method. (b) Predicted errors at $d = 1.6 \times L$. Note: Errors are expressed as mean values and bars representing the minimum and maximum values in order to illustrate the whole range of the error that could occur for each element length considering all cases.

3.3   TCD point method vs. TCD with mesh control for fretting fatigue life prediction

For the experimental results listed in **Table 3**, the estimated vs. experimental number of cycles to failure diagrams are illustrated in **Fig. 9**. The predictions were made both by means of the traditional TCD method (TCD point method) and the novel method under analysis (TCD mesh control).

(a)

(b)

(c)

(d)
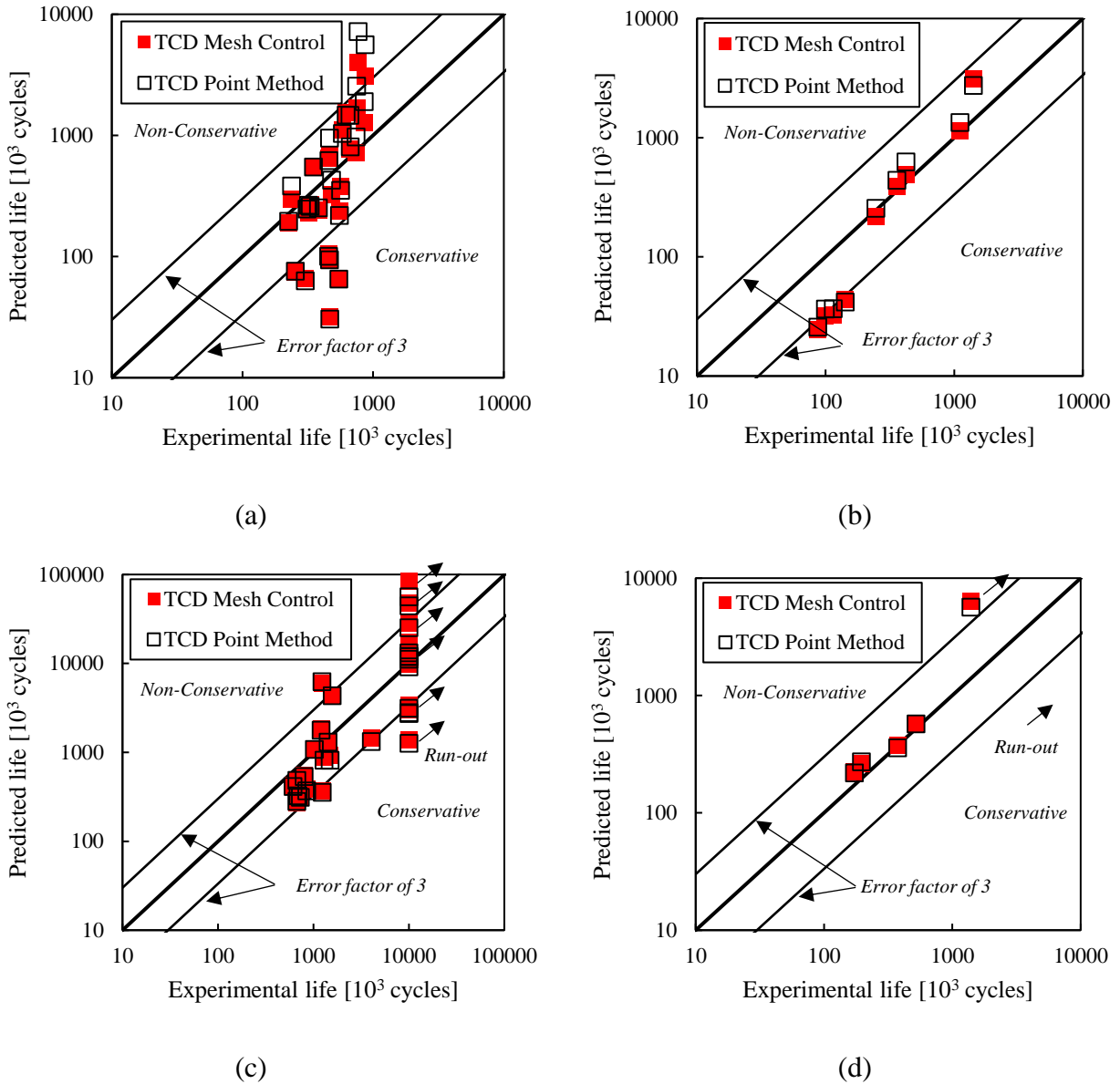
Fig. 9. Correlation between predicted and experimental lives for the TCD point method and the TCD with mesh control method for the four different data sets: (a) Al2024-T351 from Szolwinski and Farris [30];(b) Al2024-T3 from Talemi et al. [31]; (c) Al/4%Cu from Nowell [32] ;(d) Ti-6Al-4V from Araújo and Nowell [25].

There appear to be two highlights in the interpretation extracted from the obtained results: (i) the accuracy of the mesh control approach and (ii) the ability to predict life. In general, similar life

predictions were obtained by using both the traditional TCD and the TCD with mesh control. Furthermore, the error charts shown in **Fig. 6** and **Fig. 8** demonstrate that the use of both TCD approaches (traditional and mesh control) resulted in reliable predictions overall, despite the assumptions that were made to extract the material information from literature, which will be discussed later.

It should be noted that a similar prediction accuracy was achieved while significantly reducing the computing time up to 97 % (without considering the extra time required in the traditional method to generate a more refined FE model).

However, despite the promising results, some open questions remain in order to determine the range of validity for the TCD with mesh control approach applied to fretting fatigue, such as the possibility of extrapolating the selected optimum mesh size to other fatigue indicator parameters or other contact configurations, as well as applying the analysis in 3D models.

The uncertainty of the presented results related to the material input data (Basquin and critical distance parameters) taken from literature should also be noted, as these data could be slightly different from the ones used in the experimental testing. As stated by Taylor [16]: 'to date no one has carried out a TCD analysis using test data on both fretting fatigue and conventional fatigue from the same batch of material in the same laboratory, which would be necessary in order to test and apply the method with confidence'. A decade later this does not seem to have changed, since recently published studies used material properties taken from the literature [38,39]. This situation is presumably motivated by the cost of conducting the required experimental testing, and probably represents one of the drawbacks of the analysis.

Within the aforementioned limitations, the present study strongly suggests that the TCD mesh control method can be extended to non-proportional stress problems by a reasonable assumption of setting the right element size (proportional to critical distance) to overcome the current limitations of the traditional TCD method. This study highlights the immense potential for studying complex 3D industrial components and structures subjected to fretting fatigue phenomena using FEA with a reasonable effort and without resorting to complex and adaptive remeshing techniques. However, in the analysed cases, the contact zone areas were of the same order. Therefore, the influence of larger contact areas and the corresponding lower stress gradients cannot be ascertained, requiring further studies. The follow-on work will be focussed on studying a wide range of materials and contact conditions in order to determine the optimum element size. Based on the current study, the use of a d element size of $1.6 \times L$ is suggested when using a FE method for the implementation of TCD mesh control on fretting fatigue life estimation. This value could vary slightly between different FE

software packages because the internal stress averaging procedure is important and might not be the same for different FE codes.

4. Conclusions

This study analysed the viability of applying the novel TCD with mesh control approach for fretting fatigue life predictions using FEA to overcome the current limitations of the traditional TCD method. A total of seventy experimental cases using four different materials were tested as part of this research work. Based on these results, the following conclusions may be drawn:

- The TCD with mesh control approach provided similar Smith-Watson-Topper [27] (SWT) values such as the mean error = 5 %, maximum error < 12 % and similar life predictions when compared to the traditional TCD.
- The proposed method of TCD with mesh control approach gained significant computational efficiency as it reduces the simulation time up to about 97% compared to using the original TCD.
- Both approaches, the traditional TCD and TCD with mesh control, provided acceptable life predictions when compared to the experimental results.

The results obtained in the present study strongly support the conclusion that the TCD with mesh control might be used in practical situations to perform fretting fatigue assessment by simply setting an element size proportional to the critical distance ($d = 1.6 \times L$). Together with computing the life calculation at the hot spot, it allows for significant reductions in cost and time. It thus highlights the potential of studying complex 3D components and structures subjected to fretting fatigue phenomena using FEA in a cost-effective manner for industrial applications.

References

[1]   Vingsbo O, Söderberg S. On fretting maps. Wear 1988;126:131–47. doi:10.1016/0043-1648(88)90134-2.

[2]   Hills DA, Nowell D. Mechanics of Fretting Fatigue. Springer; 1994.

[3]   Anandavel K, Prakash RV. Effect of three-dimensional loading on macroscopic fretting aspects of an aero-engine blade–disc dovetail interface. Tribol Int 2011;44:1544–55. doi:10.1016/j.triboint.2010.10.014.

[4]   Cruzado A, Leen SB, Urchegui MA, Gómez X. Finite element simulation of fretting wear and fatigue in thin steel wires. Int J Fatigue 2013;55:7–21. doi:10.1016/j.ijfatigue.2013.04.025.

[5]   Ding J, Sum WS, Sabesan R, Leen SB, McColl IR, Williams EJ. Fretting fatigue predictions in a complex coupling. Int J Fatigue 2007;29:1229–44. doi:10.1016/j.ijfatigue.2006.10.017.

[6]   Han L, Chrysanthou A, O'Sullivan JM. Fretting behaviour of self-piercing riveted aluminium alloy joints under different interfacial conditions. Mater Des 2006;27:200–8. doi:10.1016/j.matdes.2004.10.014.

[7]   Hoeppner DW, Chandrasekaran V. Fretting in orthopaedic implants: A review. Wear 1994;173:189–97. doi:10.1016/0043-1648(94)90272-0.

[8]   Llavori I, Esnaola JA, Zabala A, Gomez ML and X. Fretting: Review on the Numerical Simulation and Modeling of Wear, Fatigue and Fracture. Contact Fract Mech 2017. doi:10.5772/intechopen.72675.

[9]   Nowell D, Dini D, Hills DA. Recent developments in the understanding of fretting fatigue. Eng Fract Mech 2006;73:207–22. doi:10.1016/j.engfracmech.2005.01.013.

[10]   Navarro C, Muñoz S, Domínguez J. On the use of multiaxial fatigue criteria for fretting fatigue life assessment. Int J Fatigue 2008;30:32–44. doi:10.1016/j.ijfatigue.2007.02.018.

[11]   Bellecave J. Stress Gradients In Fretting Fatigue. L'École Normale Supeériere de Cachan and Universidade de Brasilia, 2015.

[12]   Nowell D, Dini D. Stress gradient effects in fretting fatigue. Tribol Int 2003;36:71–8. doi:10.1016/S0301-679X(02)00134-2.

[13]   Navarro C, Vázquez J, Domínguez J. A general model to estimate life in notches and fretting fatigue. Eng Fract Mech 2011;78:1590–601. doi:10.1016/j.engfracmech.2011.01.011.

[14]   Vantadori S, Fortese G, Ronchei C, Scorza D. A stress gradient approach for fretting fatigue assessment of metallic structural components. Int J Fatigue 2017;101:1–8. doi:10.1016/j.ijfatigue.2017.04.004.

[15] Vázquez J, Carpinteri A, Bohórquez L, Vantadori S. Fretting fatigue investigation on Al 7075-T651 alloy: Experimental, analytical and numerical analysis. Tribol Int 2019;135:478–87. doi:10.1016/j.triboint.2019.03.028.

[16] Taylor D. The Theory of Critical Distances: A New Perspective in Fracture Mechanics. Elsevier; 2010.

[17] Bernardo AT, Araújo JA, Mamiya EN. Proposition of a finite element-based approach to compute the size effect in fretting fatigue. Tribol Int 2006;39:1123–30. doi:10.1016/j.triboint.2006.02.028.

[18] Araujo JA, Susmel L, Taylor D, Lopes LHM. Application of the Theory of Critical Distance to Fretting Fatigue. In: Gdoutos EE, editor. Fract. Nano Eng. Mater. Struct., Springer Netherlands; 2006, p. 1099–100.

[19] Taylor D. The theory of critical distances. Eng Fract Mech 2008;75:1696–705. doi:10.1016/j.engfracmech.2007.04.007.

[20] Naboulsi S, Mall S. Fretting fatigue crack initiation behavior using process volume approach and finite element analysis. Tribol Int 2003;36:121–31. doi:10.1016/S0301-679X(02)00139-1.

[21] Swalla DR, Neu RW. Characterization of Fretting Fatigue Process Volume Using Finite Element Analysis. Fretting Fatigue Adv Basic Underst Appl 2003. doi:10.1520/STP10753S.

[22] Vargiu F, Sweeney D, Firrao D, Matteis P, Taylor D. Implementation of the Theory of Critical Distances using mesh control. Theor Appl Fract Mech 2017;92:113–21. doi:10.1016/j.tafmec.2017.05.019.

[23] Fouvry S, Kapsa Ph, Vincent L. A multiaxial fatigue analysis of fretting contact taking into account the size effect. Fretting Fatigue Curr Technol Pract 2000;ASTM STP 1367:167–82.

[24] Van KD, Griveau B, Message and O. On a New Multiaxial Fatigue Limit Criterion: Theory and Application. ICBMFF2, 1998.

[25] Araújo JA, Nowell D. The effect of rapidly varying contact stress fields on fretting fatigue. Int J Fatigue 2002;24:763–75. doi:10.1016/S0142-1123(01)00191-8.

[26] Araújo JA, Nowell D, Vivacqua RC. The use of multiaxial fatigue models to predict fretting fatigue life of components subjected to different contact stress fields. Fatigue Fract Eng Mater Struct 2004;27:967–78. doi:10.1111/j.1460-2695.2004.00820.x.

[27] Smith KN, Watson P, Topper TH. A Stress-Strain Function for the Fatigue of Metals. J Mater 1970;5:767–78.

[28] Fatemi A, Socie DF. A Critical Plane Approach to Multiaxial Fatigue Damage Including Out-of-Phase Loading. Fatigue Fract Eng Mater Struct 1988;11:149–65. doi:10.1111/j.1460-2695.1988.tb01169.x.

[29] Gandiolle C, Fouvry S. Stability of critical distance approach to predict fretting fatigue cracking: a "ℓopt–bopt" concept. Int J Fatigue 2016;82:199–210. doi:10.1016/j.ijfatigue.2015.07.016.

[30] Szolwinski MP, Farris TN. Observation, analysis and prediction of fretting fatigue in 2024-T351 aluminum alloy. Wear 1998;221:24–36. doi:10.1016/S0043-1648(98)00264-6.

[31] Hojjati-Talemi R, Abdel Wahab M, De Pauw J, De Baets P. Prediction of fretting fatigue crack initiation and propagation lifetime for cylindrical contact configuration. Tribol Int 2014;76:73–91. doi:10.1016/j.triboint.2014.02.017.

[32] Nowell D. An analysis of fretting fatigue. http://purl.org/dc/dcmitype/Text. University of Oxford, 1988.

[33] MIL-HDBK-5G, Metallic Material and Elements for Aerospace Vehicle Structures. Def Print Serv Detachment Off Phila PA 1994;1.

[34] Forman RG, Shivakumar V, Cardinal JW, Williams LC, McKeighan PC. Fatigue Crack Growth Database for Damage Tolerance Analysis 2005.

[35] Hertzberg R. Deformation and Fracture Mechanics of Engineering Materials (4th edition). John Wiley & Sons, Inc. 1996.

[36] Dowling NE. Mechanical behavior of materials: engineering methods for deformation, fracture, and fatigue. 4th ed. Boston, MA: Pearson; 2012.

[37] Madge JJ, Leen SB, Shipway PH. A combined wear and crack nucleation–propagation methodology for fretting fatigue prediction. Int J Fatigue 2008;30:1509–28. doi:10.1016/j.ijfatigue.2008.01.002.

[38] Bhatti NA, Pereira K, Abdel Wahab M. Effect of stress gradient and quadrant averaging on fretting fatigue crack initiation angle and life. Tribol Int 2019;131:212–21. doi:10.1016/j.triboint.2018.10.036.

[39] Llavori I, Zabala A, Urchegui MA, Tato W, Gómez X. A coupled crack initiation and propagation numerical procedure for combined fretting wear and fretting fatigue lifetime assessment. Theor Appl Fract Mech 2019;101:294–305. doi:10.1016/j.tafmec.2019.03.005.